



PMME 2016

# Optimization of Input Parameters on Erosion Wear Rate of PTFE/HNT filled nanocomposites

G Suresh<sup>a,b,\*</sup>, V Vasu<sup>c</sup>, G Raghavendra<sup>c</sup>

<sup>a</sup>Asst. Professor, Mechanical Engineering Department, Vignan's University, Vadlamudi-522213, India

<sup>b</sup>Research Scholar, Mechanical Engineering Department, NITW, Warangal-506004, India

<sup>c</sup>Asst. Professor, Mechanical Engineering Department, NITW, Warangal-506004, India

---

## Abstract

In the current paper an extensive study on erosion wear was carried out on PTFE/HNT nanocomposites by air jet erosion tester as per ASTM G76 standard. The test was conducted on nanocomposite samples those were made with 4%, 6%, and 8% by weight of HNT in PTFE matrix. The experiments were designed in a user defined response surface methodology (RSM) and were performed on the erosion tester. The control factors used were: composition (A) with 3 levels, pressure (B) with 3 levels and impingement angle (C) with 4 levels. A full factorial design with 36 runs was planned. The results were then analyzed by using Design Expert software in response surface methodology (RSM). Analysis of variance (ANOVA) was also carried out and a quadratic model with regression equation was established. Surface plots were plotted corresponding to factors AB, BC, and AC. Conforming to the minimization of erosive wear at desirability equal to 1: 8% by weight HNT composition, 0.72 bar pressure, and 90° impingement angle were found. Also plots representing the effect of impingement angle and pressure on erosion wear rate were plotted. From the plots maximum wear was found corresponding to low impingement angles and higher operating pressures

© 2016 Elsevier Ltd. All rights reserved.

Selection and Peer-review under responsibility of International Conference on Processing of Materials, Minerals and Energy (July 29th – 30th) 2016, Ongole, Andhra Pradesh, India.

*Keywords:* Polytetrafluoroethylene matrix; Halloysite nanotubes; striking angle; erosion rate; Response Surface Methodology

---

\* This is an open-access article distributed under the terms of the Creative Commons Attribution-Non Commercial-Share Alike License, which permits non-commercial use, distribution, and reproduction in any medium, provided the original author and source are credited.

\*Corresponding author: Tel: 0863 234 4700, +919441129991

E-mail address: [gaminigsuresh@nitw.ac.in](mailto:gaminigsuresh@nitw.ac.in)

2214-7853 © 2016 Elsevier Ltd. All rights reserved.

Selection and Peer-review under responsibility of International Conference on Processing of Materials, Minerals and Energy (July 29th – 30th) 2016, Ongole, Andhra Pradesh, India.

## 1. Introduction

Solid particle erosion wear is one among the other wear modes, occurs when hard solid particles entrained in a fluid and impinging the target surface at different angles. It involves the gradual loss of material of the target surface when exposed to the dusty environments encounters in many industrial applications. This results change in functional properties and life of the components. In general there are several applications of components which are made of polymer composites working in sandy environments; situations like pipelines carrying sand, slurries in petroleum refining, helicopter rotor blades, pump impeller blades etc., If proper measures not taken to overcome the loss of material; the component cost due to wear failure will be increased because of replacement frequency. Hence many researchers worked, in order to improve the resistance to rain and sand erosion of reinforced polymers [1-4]. The erosion wear rate is a dynamic process and governed by several operating factors like, striking velocity, angle of impingement, shape and size of erodent, erodent discharge rate, erodent material properties, and target material properties[5-13].

Polytetrafluoroethylene (PTFE) is one of the iconic thermoplastic material offers a broad range operating temperatures and are used for several applications include bearing pads and compressor piston seals. [14], oven conveyor belts for food industry, and architectural protective coverings which are exposed to rain and sand erosion. [15]. A very little literature was available on PTFE and its composites in erosion wear area. The matrix material, PTFE is a semi-crystalline, high temperature resistant material and can be reusable but suffers from low wear and inferior dsmechanical properties. In order to strengthen and increase the usability with the addition of fillers/nanofillers are generally used. Halloysite nanotubes (HNTs) are naturally and abundantly available filler material at relatively low cost. A conventional method of processing of the PTFE nanocomposites in bulk is also another favourable aspect in choosing the matrix material. Design of high performance nanocomposites is highly essential to increase the wear strength, decrease the replacement costs and there by diminishes the environmental pollution and many health issues. Hence, in the current paper the work is carried out on the complex material made of PTFE and HNTs filled nanocomposites.

### Nomenclature

Q	Mass flow rate of sand particles: 2.06 gm/min
t	Test duration: 10 min
$\theta$	Impingement angle, deg.
$m_1$	Mass of sample before test, g
$m_2$	Mass of sample after test, g
$\Delta m$	$m_2 - m_1$ : Mass loss of the specimen during the test, g
M	Total mass of the sand particles striking the surface, g
$E_{wr}$	Steady state erosion wear rate, (g/g)

## 2. Martials and Methods

PTFE (INOFLON 640) powder was procured from GFL, Gujarat, with average particle size of 25 microns. Halloysite Nanotubes with alternate layers of alumina-silicate are procured from NaturalNano Inc., USA. The Halloysite nanotubes have the average dimensions of inner diameter of 20nm, outer diameter of 50nm, and lengths up to 200nm. Fig. 1(a), shows the SEM image of unmodified HNTs on 200 nm scale at 50.00 K X magnification.

### 2.1 Fabrication of nanocomposites

Conventional compression molding technique was used to fabricate the sheets (300 mm x 300 mm x 3mm) of PTFE reinforced HNT nanocomposites. Fabrication of PTFE nanocomposite sheets followed four steps viz., mixing,

preforming, sintering and cleaning. A 250 ton hydraulic compression molding press with molding pressure of 14MPa was used for production of PTFE Nanocomposite sheets. They were sintered in electrical furnace as per heating and cooling sintering cycle provided by the manufacturer as shown in Fig. 1(b). PTFE nanocomposite Sheets were fabricated with 4%, 6%, and 8% HNTs filler by weight. The samples were then cut closely to the dimensions: 25 mmx25mmx3mm from the sheets.

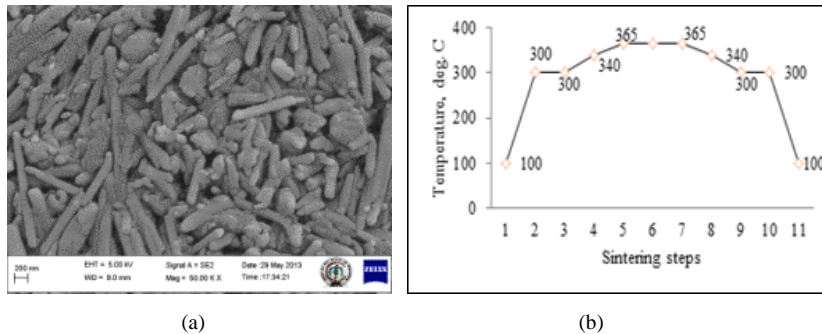


Fig. 1(a) SEM image of Unmodified HNTs at 50.0 K X magnification; (b) Sequence of heating and cooling cycles

## 2.2 Design of Experiments

Design of experiments approach is powerful tool used to analyse the relationship among the input factors known as control factors and output parameters known as response variable with minimum possible number of experiments. In the erosion field the technique was adopted by many researchers to find the optimum operating conditions to give minimum erosion wear rate [16-19]. In the present study, response surface methodology approach was adopted to meet the minimization of the erosion wear rate. Design Expert 10.0 educational version was utilized to carry out the analysis. The experiments were planned by using customized response surface method option. Table 1, shows the control factors with the corresponding levels. A full factorial design consists of total 36 experimental runs were planned.

Table 1: Control factors and levels

Control parameter	Coded parameters	Levels			
		1	2	3	4
Filler, % HNT	A	4	6	8	
Pressure, bar	B	0.5	1	1.5	
Impingement angle, degrees	C	30	45	60	90

## 2.3 Experiment Procedure

The erosive wear tests were conducted on a standard air jet erosion test rig as shown in Fig. 2. The set up was made to meet ASTM G76-83 standard. The erodent particles selected as silica sand (40-100 microns size) and were accelerated by compressed air, exiting from a tungsten carbide nozzle (length 63 mm, diameter 1.5 mm). The accelerated particles finally hit the target surface which was away from nozzle centre by 10 mm. The measurements were done according to the standard [20]. The velocity of the particles was determined as 86 m/s, 101 m/s, and 119 m/s at 0.5 bar, 1bar, and 1.5 bar respectively, by using the double disc method [21]. All the specimens were tested in the chamber at room temperature. The mass loss of the samples after erosion test ( $\Delta m$ ) was measured through a precision balance. Finally the erosion wear rate was calculated by using the equation (1). The results were presented in Table 2.

$$\text{Erosion wear rate, } E_{wr} = \frac{\Delta m}{M} \quad (1)$$

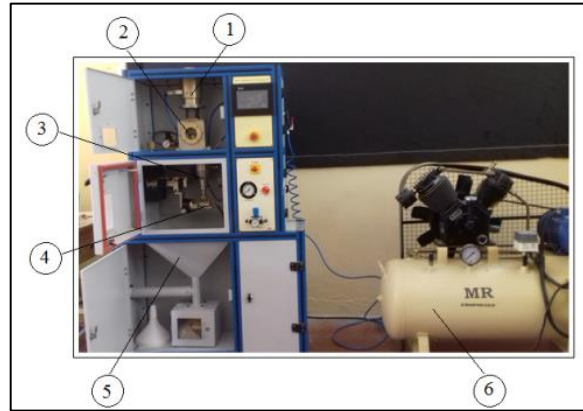


Fig. 2 Air jet erosion test set up (MAGNUM make): 1. Hopper section; 2. Conveyor belt section; 3. Mixing chamber section; 4. Specimen holder section; 5. Collecting chamber; 6. Reciprocation air compressor

### 3. Results ad Discussion

Table2: Erosion wear rate for the experimental runs

Run	Filler, %HNT	Pressure, bar	Impingement angle, $\theta^{\circ}$	$m_1$ , g	$m_2$ , g	$E_{wr}(\text{g/g}) \times 10^{-5}$
1	4	0.5	30	4.5329	4.5320	4.3689
2	4	0.5	45	4.2850	4.2842	3.8835
3	4	0.5	60	4.5318	4.5312	2.9126
4	4	0.5	90	4.2858	4.2850	3.8835
5	4	1.0	30	4.2742	4.2704	18.4466
6	4	1.0	45	4.4386	4.4343	20.8738
7	4	1.0	60	4.2704	4.2677	13.1068
8	4	1.0	90	4.4388	4.4386	0.9708
9	4	1.5	30	4.1422	4.1332	43.6893
10	4	1.5	45	4.3882	4.3792	43.6893
11	4	1.5	60	4.1332	4.1272	29.1262
12	4	1.5	90	4.4719	4.4706	6.3107
13	6	0.5	30	4.2863	4.2853	4.8544
14	6	0.5	45	4.2590	4.2577	6.3107
15	6	0.5	60	4.2853	4.2846	3.3981
16	6	0.5	90	4.2591	4.2590	0.4854
17	6	1.0	30	4.2948	4.2905	20.8738
18	6	1.0	45	4.4143	4.4100	20.8738
19	6	1.0	60	4.2905	4.2873	15.5340
20	6	1.0	90	4.4393	4.4389	1.9417
21	6	1.5	30	4.5017	4.4917	48.5437
22	6	1.5	45	4.3248	4.3151	47.0874
23	6	1.5	60	4.4917	4.4845	34.9515
24	6	1.5	90	4.3264	4.3248	7.7670
25	8	0.5	30	4.3599	4.3588	5.3398
26	8	0.5	45	4.4288	4.4273	7.2815
27	8	0.5	60	4.3588	4.3581	3.3981
28	8	0.5	90	4.4286	4.4285	0.4854
29	8	1.0	30	4.3236	4.3180	27.1845
30	8	1.0	45	4.4175	4.4128	22.8155
31	8	1.0	60	4.3180	4.3148	15.5340
32	8	1.0	90	4.4179	4.4177	0.9710
33	8	1.5	30	4.3605	4.3468	66.5049
34	8	1.5	45	4.4120	4.4003	56.7961
35	8	1.5	60	4.3468	4.3390	37.8641
36	8	1.5	90	4.4131	4.4121	4.8544

### 3.1 Response surface methodology (RSM)

In RSM a surface known as response surface which was plotted by the interaction of input factors with the output response. Fig. 3 (a) was plotted and many of studentized residuals were lying on the straight line indicating the model was a valid one. Table 3 shows a valid model obtained from ANOVA. Factors A, B, C, and their interactions AB, BC, CA, and self-interactions B<sup>2</sup> and C<sup>2</sup> were found to be significant. Fig. 3 (b) shows a close relation between actual experimental values and predicted values of erosion wear rates. A regression equation (2) in the form of mathematical model was obtained from the software and can be used to calculate any intermediate values of input factors. R-Squared value indicates the possible usage and validity of the model. Table 4 depicts a good R-squared and adjusted R-Squared values of 98.06 and 97.39 respectively.

$$\begin{aligned} \text{Erosion Rate} = & +1.496\text{E-}004 + 2.032\text{E-}005 \times \mathbf{A} + 1.445\text{E-}004 \times \mathbf{B} - 1.221\text{E-}004 \times \mathbf{C} \\ & + 2.609\text{E-}005 \times \mathbf{AB} - 3.000\text{E-}005 \times \mathbf{AC} - 1.124\text{E-}004 \times \mathbf{BC} \\ & + 6.270\text{E-}006 \times \mathbf{A}^2 + 4.814\text{E-}005 \times \mathbf{B}^2 - 3.516\text{E-}005 \times \mathbf{C}^2 \end{aligned} \quad (2)$$

Table 3: ANOVA for Response Surface Quadratic model

Source	Sum of Squares	dof	Mean Square	F Value	p-value Prob> F
<b>Model</b>	<b>1.139E-006</b>	<b>9</b>	<b>1.266E-007</b>	<b>145.98</b>	<b>&lt; 0.0001</b>
A	9.633E-009	1	9.633E-009	11.11	0.0026
B	4.874E-007	1	4.874E-007	561.98	0.0001
C	2.894E-007	1	2.894E-007	333.71	0.0001
AB	1.089E-008	1	1.089E-008	12.56	0.0015
AC	1.182E-008	1	1.182E-008	13.63	0.0010
BC	1.659E-007	1	1.659E-007	191.33	0.0001
A <sup>2</sup>	3.145E-010	1	3.145E-010	0.36	0.5522
B <sup>2</sup>	1.854E-008	1	1.854E-008	21.38	0.0001
C <sup>2</sup>	8.741E-009	1	8.741E-009	10.08	0.0038

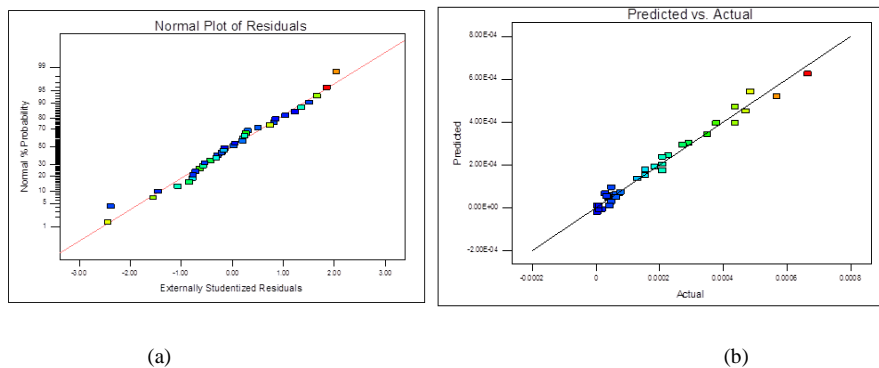


Fig. 3. (a) plot of externally studentized residuals and normal probability; (b) plot of predicted values and actual values of the test results

Table 4: Mean and R – squared values of the model

Parameter	Values
R-Squared	0.9806
Adjusted R-Squared	0.9739
Predicted R-Squared	0.9581

Significant interaction factors have considerable effect on the erosion rate was shown in Fig. 4 in terms of surface representation. From the plots Fig. 4 (a) with increasing filler %HNT (A) and pressure (B), slightly low variation in

the wear rate was found. But from other plots; Fig. 4 (b) with increasing impingement angles and operating pressure a significant increase in erosion wear rate was observed and Fig. 4 (c) increasing impingement angles and increasing filler %HNTs, a steady decrease in erosion wear rate was observed. Fig. 5 depicts the plot obtained by using MINITAB software and the optimum input factors (8 %HNT, 0.702 bar, and 90°) corresponding to a desirability of 1.0, for minimum wear rate were found.

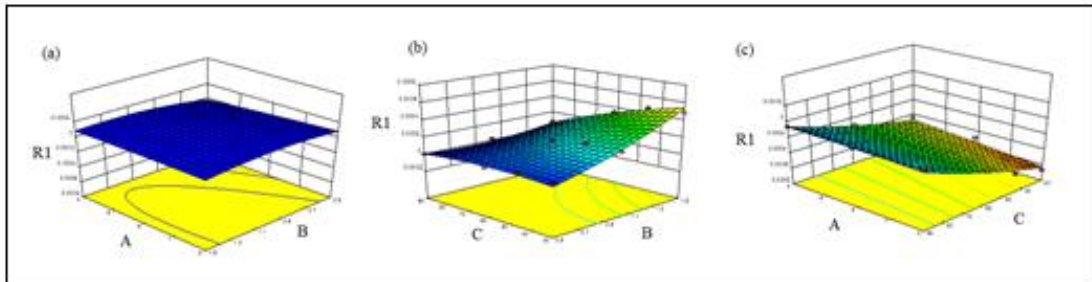


Fig. 4. Surface plots showing the combined effect of (a) AB, (b) AC, and (c) BC on erosion wear rate : R1: Erosion Wear Rate; A: Filler; B: Pressure; C: Impingement angle

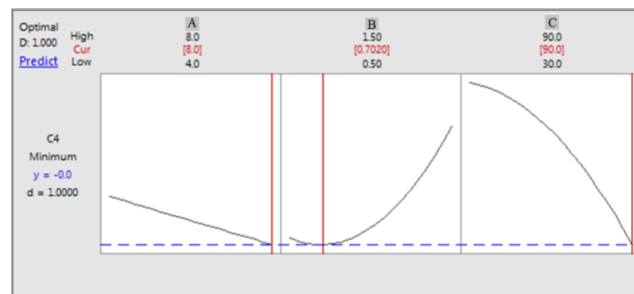


Fig. 5. Optimum operating conditions corresponding to minimum wear rate

### 3.2 Erosion wear mechanism and crater shape on the target surface

From the literature, it was known that the amount of erosion wear rate of various types of polymer matrix composites are depends upon by the amount, type, orientation and properties of the reinforcement on the one hand and by the type and properties of the matrix and its adhesion to the fibers/fillers on the other. Next to that the experimental conditions (impact angle, erodent velocity, erodent shape, erodent flux rate, etc.) have a great influence on the erosive response of the target materials. Two erosion modes are namely brittle and ductile erosion were

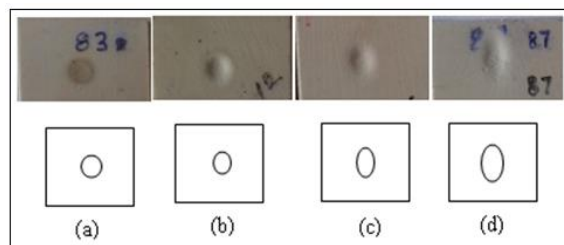


Fig. 6 Crater shape of wear at different angle of impingements:(a)  $\theta = 90^\circ$  (b)  $\theta = 60^\circ$  (c)  $\theta = 45^\circ$  (d)  $\theta = 30^\circ$ , for nano-filler addition of 8% by weight of HNT addition and at 1.5 bar pressure.

found. The erosion wear rate ( $E_{wr}$ ) of them was mainly depends on impact angle. For ductile materials  $E_{wr}$  goes through a maximum at impact angles, at about  $15^{\circ}$ – $30^{\circ}$ . For brittle materials  $E_{wr}$  continuously increases and reaches maximum at about  $90^{\circ}$ [22]. Solid particle erosion includes cutting, impact and fatigue processes. The local energy concentration of the erodent on the impacted surface was crucial for the erosive wear [23, 24]. During the impact at first the top layer consists of both matrix and reinforcement will be eroded by the cutting action and next new layer will be exposed and so on, as it was a gradual removal of material from the target surface. Also the fracture begins at the breakage of the weakest interface between the filler and matrix. Fig.6 shows the crater shape on the erosion samples at a stand-off distance of 10 mm with gradual transition of circular shape to elliptical shape with increase in the impingement angle.

3.3 Effect of individual input parameters on erosion wear rate

Fig. 7 shows the effect of pressure of air that accelerates the solid erodent particles on the erosion rate. Since the PTFE matrix material was highly ductile in nature, relatively high erosion wear rates were found corresponding to

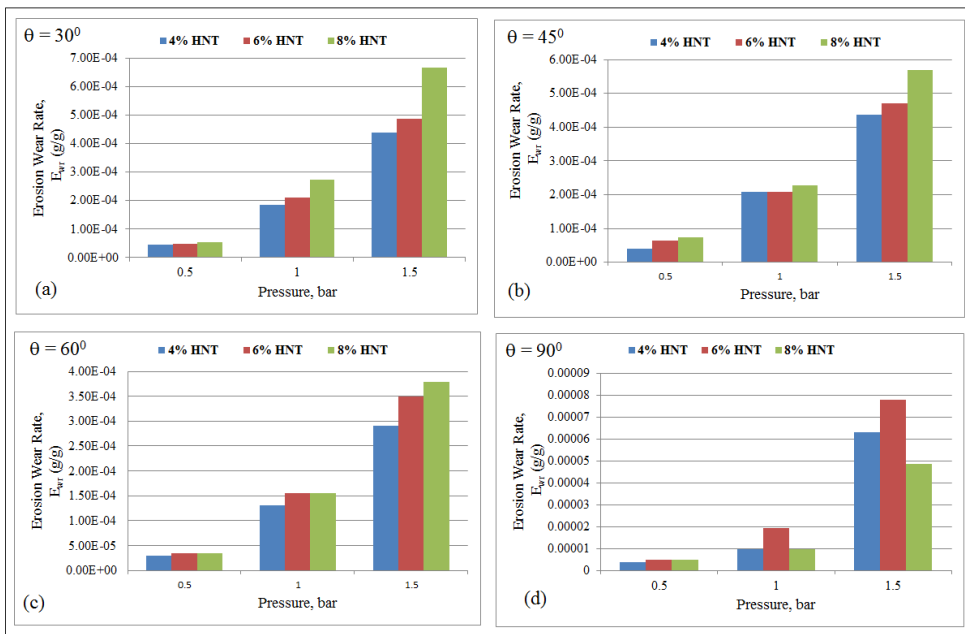


Fig. 7 the effect of pressure on erosion wear rate for different filler % inclusion in the matrix

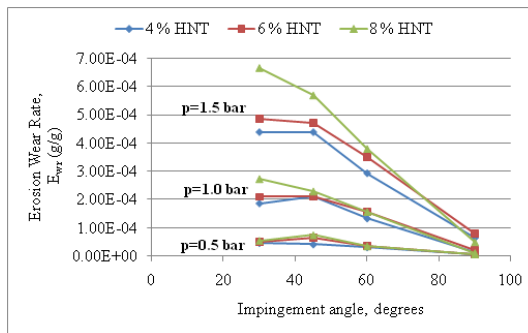


Fig. 8 the effect of impingement angles at different pressures on erosion wear rate

low impingement angles ( $30^{\circ}$  -  $45^{\circ}$ ) [22]. And gradual decrease in the wear rate was also found when impingement angle reaches  $90^{\circ}$ . From the Fig. 8, at high pressure and low impact angles an increase in the wear rate was found for all %HNT inclusions, due to micro cutting of erodent particles on the surface [22] revealing the ductile nature of the nanocomposites.

## Conclusions

- PTFE/HNT nanocomposites with 4%, 6%, 8% by weight were fabricated by using compression moulding technique
- The experiments on air jet erosion test rig were performed by using Design of Experiments technique and total 36 runs were designed for various controlling factors and levels. The velocity of particles was determined by using double disc method.
- The experimental results were then analysed by using Design Expert 10.0 and a valid model was obtained with an R-squared value of 98.06%.
- Analysis of Variance (ANOVA) was also carried out and a regression equation was formulated, showing the relationship among the input and output parameters.
- The effect of combined input parameters on the erosion rate was also studied with the help of surface plots.
- Conforming to the minimization of erosive wear at desirability equal to 1: 8% by weight HNT composition, 0,72 bar pressure, and  $90^{\circ}$  impingement angle were found.
- The effect of individual input parameters for all compositions of HNT on erosion rate was also studied from the plots. It was observed from the plots that maximum wear occurs corresponding to low impingement angles and higher operating pressures. Minimum wear rate was observed for compositions 6-8% HNT addition in the matrix material.
- The present study on PTFE/HNT nanocomposites exhibited the erosion wear mode related ductile nature.

## References

- [1] J.K. Sutter, K. Miyoshi, C. Bowman, S.K. Naik, K. Ma, R. Sinatra, R. Cupp, R. Horan, G. Leissler, *High Performance Polymers* 15 (4) (2003) 421-440.
- [2] P.V. Rao, *ASME/Fluids Engineering Publications* 23 (1995) 87-96.
- [3] S. Naik, D. Macri, J.K. Sutter, , *Proceedings of SAMPE 44th International Symposium* 44 (1) (1999) 68.
- [4] N. Dalili, A. Edrisy, R. Carriveau, 13 (2) (2009) 428-438.
- [5] W. Brandt Goldsworthy & Associates *Encyclopaedia of Polymer Science and Technology*, John Wiley & Sons, Inc. 3rd Edition - Handbook/Reference Book, ISBN-10: 0-471-27507-7, November (2004).
- [6] A.P. Harsha, U.S. Tewari, B. Venkatraman, *Wear* 254 (2003) 693-712.
- [7] T. Sinmazcelik, I. Taskiran, *Materials and Design* 28 (2007) 2471-2477.
- [8] R. Rattan, J. Bijwe, *Wear* 262 (2007) 568-574.
- [9] G.K. Drensky, Doctor of Philosophy M.S. University of Cincinnati. Cincinnati, Ohio, (2002).
- [10] N. Sari, T. Sinmazcelik, *Materials and Design* 28 (2007) 351-355.
- [11] A.P. Harsha, A.A. Thakre, *Wear* 262 (2007) 807-818.
- [12] T. Sinmazcelik, S. Fidan, V. Gunay, *Materials and Design* 29 (2008) 1419-1426.
- [13] S. Arjula, A.P. Harsha, M.K. Ghosh, *Materials Letters* 62 (2008) 3246-3249.
- [14] Bhushan, B. and Wilcock, D. F. *Wear*, 75, (1982) 41-70.
- [15] Duncan M. Pricea, Mark Jarrattb, *Thermochimica Acta* (Elsevier), 392-393 (2002) 231-236
- [16] A. Patnaik, A. Satapathy, S.S. Mahapatra, R.R. Dash, *Journal of Reinforced Plastics and Composites* 27 (8) (2008) 871-888.
- [17] A. Patnaik, A. Satapathy, S.S. Mahapatra, R.R. Dash, *Journal of Reinforced Plastics and Composites* 27 (10) (2008) 1039-1058.
- [18] A. Patnaik, A. Satapathy, S.S. Mahapatra, R.R. Dash, *Journal of Reinforced Plastics and Composites* 27 (10) (2008) 1093-1111.
- [19] A. Patnaik, A. Satapathy, S.S. Mahapatra, R.R. Dash, *Journal of Polymer Research* 15 (2) (2008) 147-160.
- [20] ASTM-G76-83: Standard practice for conducting erosion tests by solid particle impingement using gas jets (1989).
- [21] S.M. Walley, J.E. Field, *Philosophical Transactions of the Royal Society, London A* 321 (1987) 277-303.
- [22] D.R. Andrews, *Journal of Physics D: Applied Physics* 14 (1981) 1979-1991.
- [23] J.C. Arnold, I.M. Hutchings, *Journal of Physics D: Applied Physics* 25 (1992) A212-A229.
- [24] Amar Patnaik, Alok Satapathy, Navin Chand, N.M. Barkoula, Sandhyarani Biswas, *Wear* 268 (2010) 249-263 -304.